Predicting the end-stage of the COVID-19 epidemic in Brazil

W.E. Fitzgibbon[(a)] J.J. Morgan[(a)] G.F. Webb[(b)*] Y. Wu[(c)]

[(a)] *Department of Mathematics, University of Houston,*

[(b)] *Department of Mathematics, Vanderbilt University*

[(c)] *Department of Mathematics, Middle Tennessee State University*

May 28, 2020

Abstract

We develop a dynamic model of a COVID-19 epidemic as a system of differential equations. The model incorporates an asymptomatic infectious stage and a symptomatic infectious stage. We apply the model to the current COVID-19 epidemic in Brazil. We compare the model output to current epidemic data, and project forward in time possible end-stages of the epidemic in Brazil. The model emphasizes the importance of reducing asymptomatic infections in controlling the epidemic.

2000 Mathematics Subject Classification: 34, 35K65, 92B99

Keywords: asymptomatic transmission, symptomatic transmission, turning point, final size, COVID-19 epidemic in Brazil.

1 Model

The epidemic population is divided into three classes: a susceptible class S, and two infected classes I_1 and I_2, representing the asymptomatic (or low level symptomatic) infectious individuals, and symptomatic (or high level symptomatic) infectious individuals, respectively. Susceptible individuals become asymptomatically infected via contact with either asymptomatically infectious or symptomatically infectious individuals. The transmission process is modelled by the force of infection term $S\left(\tau_1 I_1 + \tau_2 I_2\right)$, which constitutes a loss rate for the susceptible class and a gain rate for the asymptomatic infected class. Asymptomatic individuals become symptomatic at rate λ. Symptomatic individuals are removed at rate γ, due to recovery, isolation, mortality, or other reasons. These elements lead to the following system of ordinary differential equations:

$$\begin{aligned}
&S'(t) = -S(t)\left(\tau_1 I_1(t) + \tau_2 I_2(t)\right),\ t \geq 0,\\
&I_1'(t) = S(t)\left(\tau_1 I_1(t) + \tau_2 I_2(t)\right) - \lambda I_1(t),\ t \geq 0,\\
&I_2'(t) = \lambda I_1(t) - \gamma I_2(t),\ t \geq 0,\\
&S(0) > 0,\ I_1(0), I_2(0) \geq 0.
\end{aligned} \tag{1.1}$$

A flow diagram of the model is given in Figure 1. We remark that a model similar to (1.1) is developed in [10, 11, 12, 13], where I_2 is further differentiated into reported and unreported classes. The global dynamics of (1.1) are given in the following theorem:

Theorem 1.1 *Suppose $\tau_1 > 0, \tau_2 > 0, \lambda > 0$, and $\gamma > 0$. Then (1.1) has bounded nonnegative solutions $S(t)$, $I_1(t)$, $I_2(t)$ for $t \geq 0$, and*

$$\lim_{t\to\infty} S(t) = S_\infty > 0 \text{ and } \lim_{t\to\infty} I_i(t) = 0 \text{ for } i = 1, 2.$$

This result is proved in greater generality in [9], in a setting with S, I_1 and I_2 spatially dependent, and their equations replaced by reaction-diffusion equations over a geographical domain. For the spatially homogeneous case in Theorem 2.1, we can express S_∞ in terms of the initial conditions and parameters in the model (1.1):

*Corresponding author

Corollary 1.2 *S_∞ satisfies the following equation:*

$$S_\infty = S(0)\, exp\Big[- \Big(S(0) + I_1(0) + I_2(0) - S_\infty \Big) \Big(\frac{\tau_1}{\lambda} + \frac{\tau_2}{\gamma} \Big) - \frac{\tau_1}{\lambda} I_2(0) \Big]. \tag{1.2}$$

Proof. From the first equation in (1.1) we obtain

$$\begin{aligned} S(t) &= S(0)\, exp\Big[- \tau_1 \int_0^t I_1(s)ds - \tau_2 \int_0^t I_2(s)ds \Big] \\ \Rightarrow S_\infty &= S(0)\, exp\Big[- \tau_1 \int_0^\infty I_1(s)ds - \tau_2 \int_0^\infty I_1(s)ds \Big]. \end{aligned} \tag{1.3}$$

From the sum of the first, second, and third equation in (1.1) we obtain

$$\begin{aligned} S'(t) + I_1'(t) + I_2'(t) &= -\gamma I_2(t) \\ \Rightarrow \int_0^\infty I_2(s)ds &= \frac{S(0) + I_1(0) + I_2(0) - S_\infty}{\gamma} \end{aligned} \tag{1.4}$$

From the third equation in (1.1) we obtain

$$\begin{aligned} I_2(t) - I_2(0) &= \lambda \int_0^t I_1(s)ds - \gamma \int_0^\infty I_2(s)ds \\ \Rightarrow \int_0^\infty I_1(s)ds &= \frac{\gamma \int_0^\infty I_2(s)ds - I_2(0)}{\lambda}. \end{aligned} \tag{1.5}$$

Then, (1.2) follows from (1.3), (1.4), and (1.5). ■

2 COVID-19 in Brazil

We apply this result to the COVID-19 epidemic in Brazil. Other models of the COVID-19 epidemic in Brazil are in [1, 2, 3, 4, 5, 6, 7, 8, 14, 15, 16, 17, 18]. Currently, the epidemic in Brazil is in a rapid growth phase, with limited social distancing measures in effect, and limited compliance with these measures. We use the cumulative daily reported cases data for this epidemic from the Ministério da Saúde of Brazil (https://coronavirus.saude.gov.br/):

17	18	19	20	21	22	23	24	25	26	27
291	428	621	904	1128	1546	1891	2201	2433	2915	3417
28	29	30	31							
3903	4256	4579	5717							

Table 1: *March - cumulative reported cases in Brazil.*

1	2	3	4	5	6	7	8	9	10
6834	7910	9056	10278	11130	12056	13717	15927	17857	19638
11	12	13	14	15	16	17	18	19	20
20727	22169	23430	25262	28320	30425	33682	36599	38654	40581
21	22	23	24	25	26	27	28	29	30
43079	45757	49492	52995	58509	61888	66501	71886	78162	85380

Table 2: *April - cumulative reported cases in Brazil.*

We set the time units to days. We view $I_1(t)$ as the population of asymptomatic or low level symptomatic infectious individuals at time t. We view $I_2(t)$ as the population of high level symptomatic infectious individuals at time t. We set $S(0) = 210,000,000$, the current population of Brazil. We set the loss rate λ of $I_1(t)$ to $1/7$ per day, which means I_1 infectiousness lasts 7 days on average. We set the loss rate γ of $I_2(t)$ to $1/7$ per day, which means I_2 infectiousness lasts 7 days on average. We identify an interval of time

1	2	3	4	5	6	7	8	9
91299	96396	101147	107780	114715	125218	135106	145328	155939
10	11	12	13	14	15	16	17	18
162699	168331	177589	188974	202918	218223	233142	241080	254220
19	20	21	22	23	24	25	26	27
271628	291579	310087	330890	347398	363211	374898	391222	411821

Table 3: *May - cumulative reported cases in Brazil.*

$[t_0, t_1]$ on which the cumulative daily reported cases data is growing: $t_0 = 1$, corresponding to March 17 and $t_1 = 72$, corresponding to May 27.

The cumulative number $I_1(t)$ of low level infectious cases as a function of time t is $\int_{t_0}^{t} S(s)\,(\tau_1 I_1(s) + \tau_2 I_2(s))ds$. The cumulative number $I_2(t)$ of high level infectious cases as a function of time t is $\lambda \int_{t_0}^{t} I_1(s)ds$. The high level infectious cases I_2 are removed at the rate γ per day. We assume that a fraction $f = 0.3$ of these removed cases are reported, isolated, and cause no further transmissions. Thus, the cumulative number of reported cases at time t is $f\,\gamma \int_{t_0}^{t} I_2(s)ds$, with $f = 0.3$ and $\gamma = 1/7$. Other fractional values f could be assumed, but currently this fractional value is not known.

We fit the parameters τ_1, τ_2, and initial values $I_1(t_0)$, $I_2(t_0)$, so that the solutions of (1.1) align with the cumulative reported cases data on the time interval $[t_0, t_1]$. For this time interval, we estimate $\tau_1 = 2.5 \times 10^{-10}$, $\tau_2 = 1.0 \times 10^{-9}$, $I_1(t_0) = 13,000$, $I_2(t_0) = 8,500$, by fitting the solutions of (1.1) to the cumulative reported cases data between March 17 and May 27. This means that 25% of transmissions are due to I_1 asymptomatic or low level symptomatic cases. In Figure 2 we graph the cumulative reported cases data and the cumulative reported cases from the simulation of the model. Other choices of the parameters and initial values are possible.

The daily reported cases from the model simulation, with $f = 0.3$, $\gamma = 1/7$, $t_0 = 1$ (March 17), is obtained by solving the differential equation

$$DR'(t) = f\,\gamma\, I_2(t) - DR(t), t \geq t_0, \;\; DR(t_0) = DR_0 = 291.$$

In Figure 3 we graph the daily reported cases data and the daily reported cases from the model simulation with $f = 0.3$, $\gamma = 1/7$ and $t_0 = 1$ (March 17).

We project forward in time the model simulation of the cumulative reported cases $0.3\,\gamma \int_{t_0}^{t} I_2(s)ds$, as well as the model simulation of the total cumulative $I_1(t)$ cases $\int_{t_0}^{t} (\tau_1 I_1(s) + \tau_2 I_2(s))S(s)ds$ and the model simulation of the total $I_2(t)$ cases $\int_{t_0}^{t} \lambda I_1(s)ds$, in Figure 4. The final size of the epidemic is approximately $157,000,000$ cases. The turning points of the cumulative cases are the times at which the graphs transition from concave up to concave down. The turning points are obtained by setting the second derivative of these graphs to 0. The turning points are graphed as vertical lines. The turning point of the cumulative I_2 cases is approximately one week later than the turning point of the cumulative I_1 cases, which is consistent with the assumption that the average time of I_1 infectiousness $1/\lambda = 7$ days. The turning point of the reported cumulative I_2 cases is approximately one week later than the turning point of the cumulative I_2 cases, which is consistent with the assumption that the average time of I_2 infectiousness $1/\gamma = 7$ days.

The extremely high number of cases projected in the simulation, with an on-going unaltered transmission rate, is very unlikely. It is certain that government imposed and socially adopted distancing measures would take effect, and mitigate transmission. The formula (1.2) for S_∞ in Corollary 1.2 can be used to estimate the effects of these mitigations. The values of the initial conditions in formula (1.2) can be reset to up-dated values, with modified parameters $\lambda, \gamma, \tau_1, \tau_2$, to give forward time predictions of the final size $S_0 - S_\infty$.

In Figure 5 we graph the final size $S_0 - S_\infty$ as a function of $1/\lambda$ and $1/\gamma$. If the average number of days low level infectious individuals I_1 remain infectious is reduced to 4, and the average number of days high level infectious individuals I_2 remain infectious is reduced to 4, then the final size $S(0) - S_\infty$ of the epidemic is approximately $20,000,000$ cases. In Figure 6 we graph the final size $S_0 - S_\infty$ as a function of the I_1 transmission rate τ_1 and the I_2 transmission rate τ_2. If the transmission rate τ_1 of low level infectious individuals I_1 is reduced to 1.5×10^{-10}, and the transmission rate τ_2 of high level infectious individuals I_2 is reduced to 0.6×10^{-9}, then the final size $S(0) - S_\infty$ of the epidemic is approximately $38,000,000$ cases.

3 Conclusions

We have developed a dynamic model of a COVID-19 epidemic outbreak in a susceptible population. Our model describes the outbreak as a growth of transmission of susceptible individuals from two classes of infectious individuals: I_1 asymptomatic (low level symptomatic), and I_2 symptomatic (high level symptomatic). The model does not assume that major government measures or social behaviour changes have been implemented to mitigate the epidemic transmission. The model also assumes that reported cases are a fraction of the total cases in the population.

We apply the model to the COVID-19 current in Brazil. We identify parameters and initial conditions that give agreement of the model output with current case data from Ministério da Saúde of Brazil. We project forward in time the model solutions, to give final size predictions of the epidemic in the absence of social distancing measures. The extreme scenario that the epidemic continues, without social distancing mitigation, is extremely unlikely, given the magnitude of this final size. Intervention measures, such as isolation and contact tracing of high level symptomatic I_2 cases, and quarantining of low level symptomatic I_1 cases, can be quantified in terms of the final size formula (Corollary 2.2) of the epidemic. The reduction of $1/\gamma$ and τ_2, corresponds to the identification and isolation of I_2 high level symptomatic cases. The reduction of $1/\lambda$ and τ_1, corresponds to the contact tracing of I_2 high level symptomatic cases and quarantining of contact traced I_1 asymptomatic or low level symptomatic cases. Both measures have major effect in controlling the epidemic.

References

[1] L. R. P. de Alcantara, L. Silva, A. R. de Alcantara, *et al.*, Using different epidemiological models to modeling the epidemic dynamics in Brazil, medRxiv 2020.04.29.20085100; doi: https://doi.org/10.1101/2020.04.29.20085100.

[2] G.B. de Almeida, T. Vilches, C. Ferreira, *et al.*, Several countries in one: a mathematical modeling analysis for COVID-19 in inner Brazil, medRxiv 2020.04.23.20077438.

[3] A. Arenas, W. Cota, J. Gómez-Gardeñes *et al.*, A mathematical model for the spatiotemporal spreading of COVID-19, medRxiv, doi: https://doi.org/10.1101/2020.03.21.20040022.

[4] S.B. Bastos and D.O. Cajueiro, Modeling and forecasting the early evolution of the Covid-19 pandemic in Brazil, arXiv preprint arXiv:2003.14288, 2020.

[5] A. Canabarro, E. Tenorio, R. Martins, *et al.*, Data-driven study of the COVID-19 pandemic via age-structured modelling and prediction of the health system failure in Brazil amid diverse intervention strategies, medRxiv 2020.04.03.20052498; doi: https://doi.org/10.1101/2020.04.03.20052498.

[6] C. Castilho, J. A. M. Gondim, M. Marchesin, and M. Sabeti, Assessing the efficiency of different control strategies for the coronavirus (COVID-19) epidemic, arXiv:2004.03539v1 [q-bio.PE]

[7] R.M. Cotta, C.P. Naveira-Cotta, and P. Magal, Parametric identification and public health measures influence on the COVID-19 epidemic evolution in Brazil, medRxiv 2020.03.31.20049130; doi: https://doi.org/10.1101/2020.03.31.20049130.

[8] N. Crokidakis, Data analysis and modeling of the evolution of COVID-19 in Brazil, https://www.researchgate.net/publication/340270886.

[9] W.E. Fitzgibbon, J.J. Morgan, G.F. Webb, and Y. Wu, Analysis of a reaction-diffusion disease model with asymptomatic transmission, submitted for publication.

[10] Z. Liu, P. Magal, O. Seydi, and G.F. Webb, Understanding unreported cases in the 2019-nCov epidemic outbreak in Wuhan, China, and the importance of major public health interventions, *MPDI Biology*, (2020), 9(3), 50.

[11] Z. Liu, P. Magal, O. Seydi, and G.F. Webb, Predicting the cumulative number of cases for the COVID-19 epidemic in China from early data, *Math. Biosci. Eng.*, 17(4) (2020), 3040–3051.

[12] Z. Liu, P. Magal, O. Seydi, and G.F. Webb, A COVID-19 epidemic model with latency period, *Infect. Dis. Mod.*, 5 (2020), 323–337.

[13] Z. Liu, P. Magal, O. Seydi, and G.F. Webb, A model to predict COVID-19 epidemics with applications to South Korea, Italy, and Spain , *SIAM News*, May (2020).

[14] O.P. Neto, J.C. Reis, A.C.E. Brizzi, *et al.*, COVID-19 mathematical model reopening scenarios for São Paulo - Brazil, medRxiv preprint.

[15] J.H. Sales, Epidemic COVID mathematical model, *Int. J. Lat. Res .Sci. Tech.*, 72(2) (2020),1–5.

[16] P. Savi, M.A. Savi, and B. Borges, A mathematical description of the dynamics of the coronavirus disease 2019 (COVID-19): a case study of Brazil, http://arxiv.org/abs/2004.03495.

[17] R.A. Schulz, C.H. Coimbra-Araújo, and S.W. Costiche, COVID - 19: A model for studying the evolution of contamination in Brazil, arXiv.org > q-bio > arXiv:2003.13932.

[18] G.L. Vasconcelos, A.M.S. Macêdo, R.l. Ospina, *et al.*, Modelling fatality curves of COVID-19 and the effectiveness of intervention strategies, medRxiv 2020.04.02.20051557; doi: https://doi.org/10.1101/2020.04.02.20051557.

Figures

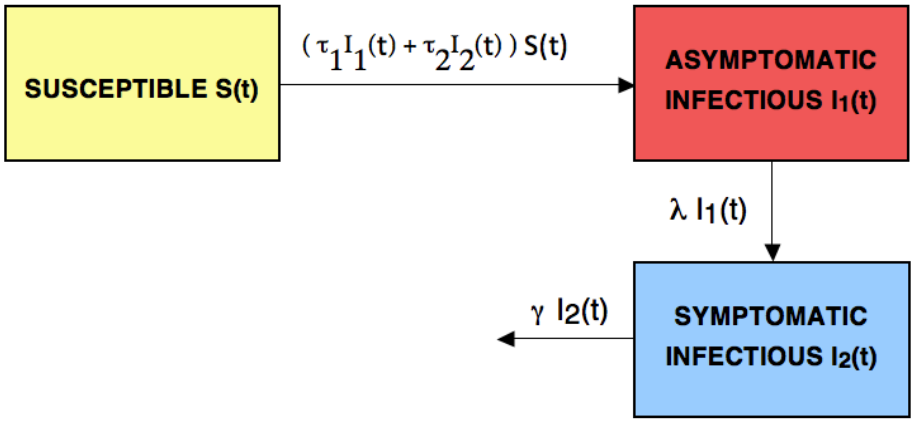

Figure 1: Flow diagram of the model.

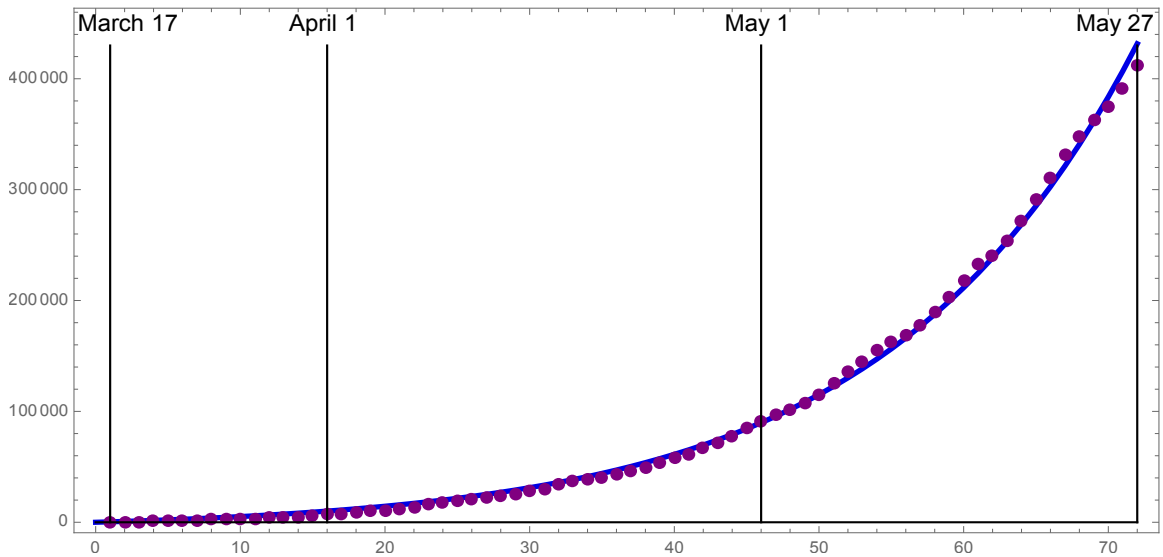

Figure 2: Dots: cumulative reported cases data from Tables 1,2,3. Graph: model simulation of the cumulative reported cases $f\,\gamma\,\int_{t_0}^{t} I_2(s)ds$, with $f = 0.3$ and $\gamma = 1/7$. f is the fraction of removed I_2 cases that are reported.

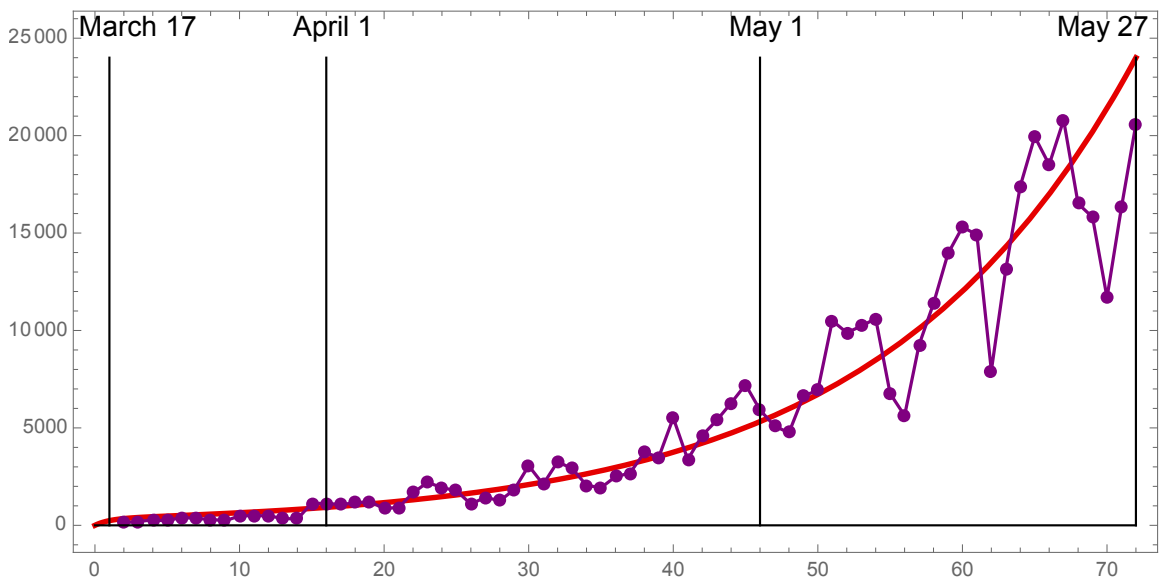

Figure 3: Dots: daily reported cases data obtained by subtraction day by day from the data in Tables 1,2,3. Graph: model simulation of the daily reported cases $DR(t)$ with $f = 0.3$, $\gamma = 1/7$, and $t_0 = 1$ (March 17).

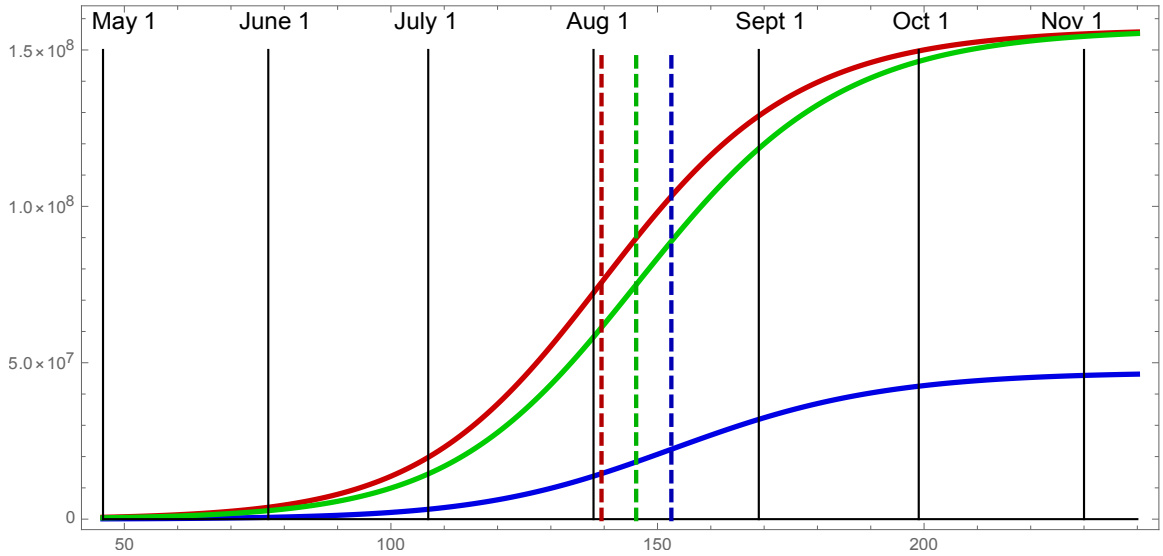

Figure 4: Blue: model simulation of the cumulative reported cases. Red: model simulation of the cumulative I_1 infectious cases. Green: model simulation of the cumulative I_2 infectious cases. The turning point of the cumulative reported cases is approximately day 152.6, the turning point of the cumulative I_1 cases is approximately day 139.5, and the turning point of the cumulative I_2 cases is day 146. The $\lim_{t\to\infty} I_2(t)$ is approximately $157,000,000$ cases.

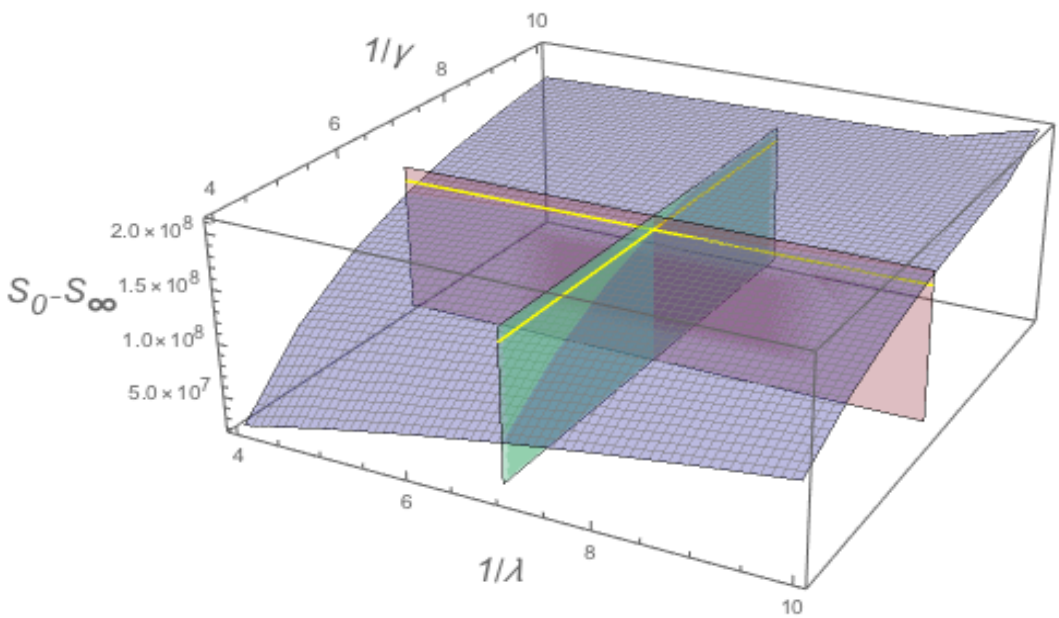

Figure 5: Blue surface: final size $S_0 - S_\infty$ graphed as a function of $1/\lambda$ and $1/\gamma$. The yellow lines and red and green planes correspond to the baseline values $\lambda = 1/7$, $\gamma = 1/7$, $S_0 - S_\infty = 157,000,000$. The final size $S(0) - S_\infty$ decreases greatly as $1/\lambda$ decreases and as $1/\gamma$ decreases. For $1/\lambda = 4$ and $1/\gamma = 4$, the final size $S(0) - S_\infty$ is approximately $20,000,000$.

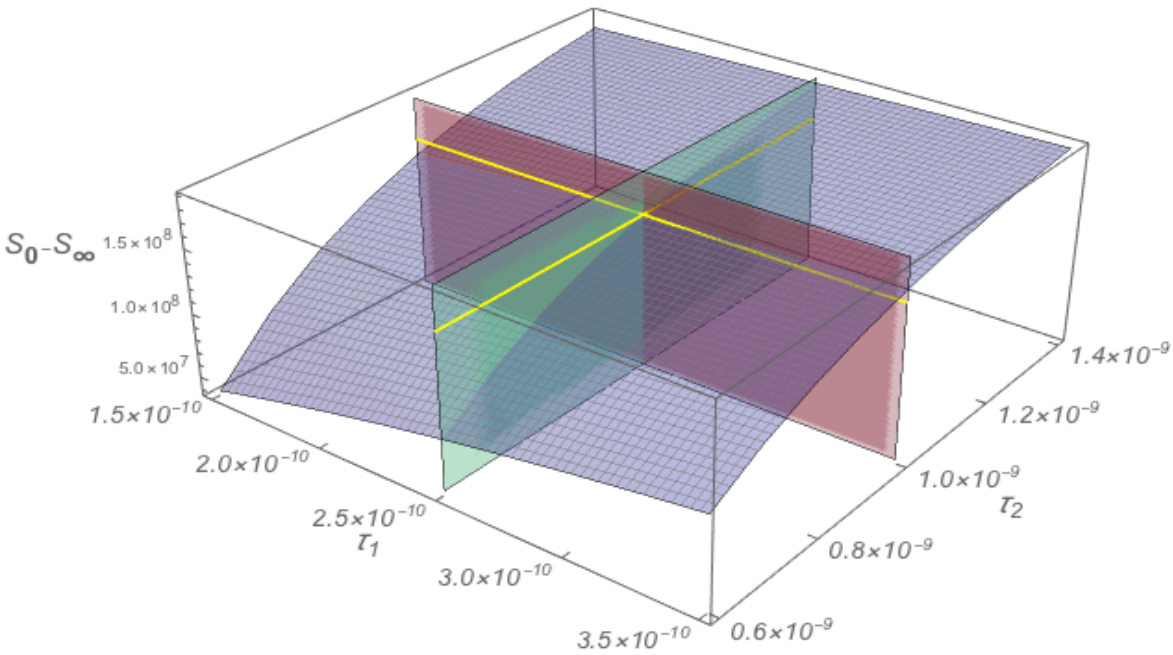

Figure 6: Blue surface: final size $S_0 - S_\infty$ graphed as a function of τ_1 and τ_2. The yellow lines and red and green planes correspond to the baseline values $\tau_1 = 2.5 \times 10^{-10}$, $\tau_2 = 1.0 \times 10^{-9}$, $S_0 - S_\infty = 157,000,000$. The final size $S(0) - S_\infty$ decreases greatly as τ_1 decreases and as τ_2 decreases. For $\tau_1 = 1.5 \times 10^{-10}$ and $\tau_2 = 0.6 \times 10^{-9}$, the final size $S(0) - S_\infty$ is approximately $38,000,000$.